Daily extreme precipitation and trends over China

SUN Jun[1,2*] & ZHANG FuQing[2†]

[1] *National Meteorological Center, China Meteorological Administration, Beijing 100081, China;*
[2] *Department of Meteorology and Atmospheric Sciences, and Center for Advanced Data Assimilation and Predictability Techniques, Pennsylvania State University, University Park, PA 16801, USA*

Abstract   Based on daily precipitation data of more than 2000 Chinese stations and more than 50 yr, we constructed time series of extreme precipitation based on six different indices for each station: annual and summer maximum (top-1) precipitation, accumulated amount of 10 precipitation maxima (annual, summer; top-10), and total annual and summer precipitation. Furthermore, we constructed the time series of the total number of stations based on the total number of stations with top-1 and top-10 annual extreme precipitation for the whole data period, the whole country, and six subregions, respectively. Analysis of these time series indicate three regions with distinct trends of extreme precipitation: (1) a positive trend region in Southeast China, (2) a positive trend region in Northwest China, and (3) a negative trend region in North China. Increasing (decreasing) ratios of 10–30% or even >30% were observed in these three regions. The national total number of stations with top-1 and top-10 precipitation extremes increased respectively by 2.4 and 15 stations per decade on average but with great inter-annual variations. There have been three periods with highly frequent precipitation extremes since 1960: (1) early 1960s, (2) middle and late 1990s, and (3) early 21st century. There are significant regional differences in trends of regional total number of stations with top-1 and top-10 precipitation. The most significant increase was observed over Northwest China. During the same period, there are significant changes in the atmospheric variables that favor the decrease of extreme precipitation over North China: an increase in the geopotential height over North China and its upstream regions, a decrease in the low-level meridional wind from South China coast to North China, and the corresponding low moisture content in North China. The extreme precipitation values with a 50-year empirical return period are 400–600 mm at the South China coastal regions and gradually decrease to less than 50 mm in Northwest China. The mean increase rate in comparison with 20-year empirical return levels is 6.8%. The historical maximum precipitation is more than twice the 50-year return levels.

Keywords   Extreme precipitation (EP), Extreme precipitation event (EPE), Time series, Total annual number of stations, Extreme event return level

1.   Introduction

Extreme precipitation events (EPEs) refer to precipitation events with low occurrence frequency at a given place in history. Once they happen, they often cause serious economic losses and even the loss of lives through secondary disasters such as floods, mudslides, landslides, and city waterlogging.

Such EPEs can occur worldwide. During the past several years, EPEs and secondary disasters greatly affected many locations in Europe, America, and Asia (e.g., Gochis et al., 2015; Moore et al., 2012; Lynch and Schumacher, 2014; Houze Jr. et al., 2011; Martius et al., 2013; Bissolli et al., 2011; Grams et al., 2014; Takahashi et al., 2015). China is significantly affected by the East Asian monsoon. Torrential rainfall often occurs when the summer monsoons burst, advance northward, and prevail in China (Tao, 1980). Several notorious EPEs have greatly damaged local areas

*Corresponding author (email: sunjun@cma.gov.cn)
† Corresponding author (email: fzhang@psu.edu)

in China in recent years. The Jilin flood occurring from the end of July to the beginning of August in 2010 in the Jilin Province was caused by ten sequential heavy rainfall events, where the daily maximum rainfall at the national (regional) station reached 388 mm (507 mm; Sun et al., 2011). The serious Zhouqu debris flow disasters in Zhouqu County, Gansu Province, in China on August 8, 2010, were also caused by a localized EPE (Tang et al., 2011; Ren, 2014). The torrential rainfall over Beijing and surrounding areas on July 21, 2012, is a typical EPE. The precipitation at 11 of 20 national weather stations over the Beijing region broke the daily precipitation record, 79 people lost their lives, and the estimated total economic losses are over 10 billion RMB (Sun et al., 2012; Chen et al., 2012; Du J et al., 2014). The floods in the Sichuan Basin from early to mid-July in 2013 were caused by continuous heavy precipitation. The total accumulated rainfall in Dujiangyan from July 8 to 11 reached an extreme value of 721.4 mm (Wang Q et al., 2013). Because of frequent disasters induced by EPEs in recent years, EPs and their trends in China have attracted much attention. It is thus of great importance to analyze Chinese EPEs and their statistical trends.

A single EPE may not contribute to climate change; however, because many EPEs have occurred in recent years, the influence of climate change should be discussed. It has been suggested that the frequency and intensity of EPEs increase due to global warming. Based on 16 simulations of the Coupled Model Intercomparison Project Phase 5 (CMIP5) for the medium and high radiative forcing scenarios (RCP4.5 and RCP8.5), consistent precipitation changes project that rainfall events in China will significantly increase and become much more extreme by the end of the 21st century (Chen, 2013). The results of analyses of 14 CMIP5 model projections indicate a robust, canonical global response of the precipitation features to CO_2 warming, that is, an increase in heavy rain (monthly mean >9 mm day^{-1}), reduction in moderate rain, and increase in light rain. The probability of extreme heavy rain (monthly mean >25 mm day^{-1}) will increase globally by 100–250% for a scenario of 1% CO_2 increase per year. The increase in heavy rainfall is most pronounced in the equatorial Central Pacific and Asian monsoon regions (Lau et al., 2013). The daily rainfall of the multi-model mean of CMIP5 is characterized by an increase of 1 % K^{-1} at all rain rates and a shift to higher rain rates of 3.3 % K^{-1} in response to CO_2 doubling. Some models also show a substantial increase in the extreme rainfall mode in response to warming (Pendergrass and Hartmann, 2014). Based on research of the relation between rainfall extremes and naturally driven changes in the surface temperature using satellite observations and model simulations, it was predicted that heavy rainfall events will increase during warm periods and decrease during cold periods (Allan and Soden, 2008). It is therefore very important to determine the correlation of global warming and EPEs in China.

The EPE trend for the whole country or certain regions of China was documented in many previous studied. The number of EPEs and average amount and intensity of EP are increasing in China (Zhai et al., 2007). The study of Zhai et al. (2007) also showed that the changes of the extreme and total precipitation correlate. The increase of total precipitation is mainly caused by the increase of the amount of EP (Min and Qian, 2008); the EP amount can contribute 1/3 of the annual total precipitation in China and dominates the trends of changing precipitation (Sun, 2012). The changes of summer EP and total summer precipitation are similar. Increase was observed in parts of Yangtze-Huaihe River Basin and in the south and southwest of China, but decrease was observed in the north and northwest of China (Zeng and Lu, 2015). The change of the annual EPE frequency is consistent with that of the summer frequency (Chen et al., 2009). The EPE trends have different characteristics in distinct regions of China. The EP amount increased in Northwest China and in the middle and lower reaches of the Yangtze River, whereas it decreased in North China and the Sichuan Basin (Zhai et al., 2005). These differences are consistent with trends of the EPEs frequency (Zou et al., 2009). Wang et al. (2014) found that the changing EP amount and its proportion of total precipitation increase in the north of eastern China and decrease in the south of eastern China, especially in North China and in the middle and lower reaches of the Yangtze River. Notable increases in the summer total precipitation and number of rainstorm days and a slight increase in the intensity of EP were observed in the middle and lower reaches of the Yangtze River (Su et al., 2006). At most of the observation stations of the North China Plain EPE trends are not notable, while significant decreases were reported for Beijing and neighboring areas (Fan et al., 2012). Changes in the days with heavy and torrential rainfall were not noted in the middle regions of North China (Zhang et al., 2008). The EPE frequency in the flood season remarkably increases in the north of Xinjiang, south of Xinjiang, Qinghai Plateau, and Hetao area and decreases in the east of Northwest China; however, no notable change was observed in the east of the Qinghai-Xizang Plateau (Yang et al., 2007). In the Xinjiang region, 70% of the observation stations indicate an increase of the EP intensity. These stations are mainly located in northern Xinjiang and in the north of southern Xinjiang (Jiang et al., 2013). The EPE changes in the southwest of China are very complex and have distinct regional features. The EP markedly increases in the mountainous region of southwestern Sichuan, while it decreases in the northwest and south of the basin. In the north of the Western Sichuan Plateau, the EP frequency increases but its intensity weakens in the middle of the Sichuan Basin (Zhang and Ma, 2011). Most EP indices of most of the stations in the Sichuan Province decrease. Especially, the total annual precipitation in wet days and the maximum number of con-

secutive wet days show significant negative trends (Huang et al., 2014). The EPE trends of other regions of China were also studied and meaningful results were obtained (Wang B L et al., 2013; Cao and Pan, 2014; Du H et al., 2014; Yang et al., 2010).

Generally, two common methods are used to define EPEs (Solomon et al., 2007; Zhai et al., 2007; Feng et al., 2010). One is the threshold method in which precipitation events with a precipitation amount exceeding a certain threshold are defined as extreme events. The second is the percentile method in which daily precipitation is sorted and classified as extreme when exceeding a certain percentile. These two methods have a common deficit if all rain days are considered, that is, when a threshold or percentile is selected, the number of precipitation events exceeding that threshold or percentile distinctly varies in different regions. For example, for a daily precipitation threshold of 50 mm, many events are defined as EPEs in the south of China, whereas few events satisfy this threshold in the west of China. Therefore, the EPEs at different observation stations in different regions are not comparable. Moreover, the data stations used in previous studies of EPs in China are very sparse. There are 700 stations nationwide at most; therefore, regional features of EP trends cannot be clearly detected. This work aims to provide an overview of EP trends in China. The dataset used in our study to investigate regional EPE features consists of data from more than 2000 Chinese observation stations and is therefore based on a much denser station network than before.

2. Data and methods

2.1 Data

The daily dataset of the China National Basic Surface Meteorological elements (V3.0) developed by the National Meteorological Information Center (NMIC) of the China Meteorological Administration was used in this study. The dataset contains data from 2480 meteorological surface observation stations from January 1, 1951, to July 31, 2012. The dataset was subjected to a series of strict quality control processes by the NMIC before publication including a climate range limits or allowable values check, station extreme value check, internal consistency check, time consistency check, and space consistency check. We extracted daily precipitation data from the dataset which is from 20Z Beijing Time the previous day to 20Z the observation day (12 UTC to 12 UTC). To use the latest data available at the study time, real-time operational daily precipitation data from August 1, 2012, to December 31, 2013, were added to the dataset. The final precipitation data were manually reexamined, and subsequently recording mistakes, such as errors in the station starting time and station ID, were identified and corrected. After above-mentioned quality control processes, daily precipitation data used in this study were reliable and accurate. The accuracy rates reach 100%.

Meteorological surface observation stations have been built since the 1950s in China. The number of stations has increased rapidly from 182 stations in 1951 to 2088 stations in 1961. After 1960, the number of stations remained relatively constant at ~2400. Therefore, the data observation time spans vary widely from station to station. The longest time span is 63 yr, whereas the shortest time span is less than 10 yr. Because this research involves statistics of the number of EP stations for each year, a relatively constant number of observation stations is needed. Therefore, we only selected data after 1960 because they are relatively complete and the number of stations is relatively large. Two criteria were applied to each station to reject stations with a lot of missing values: (1) For annual data, if a year shows missing precipitation for more than 5% of the days (20 days), that year will be considered as having inadequate observations and will be omitted. For the summer (June to August) data, if a summer shows missing data for more than 5 days, that summer will be removed; and (2) Stations with data of less than 50 yr are excluded. Finally, the dataset including data from 2024 stations for the whole year and from 2046 stations for the summer during the period from 1961–2013 was retained. The full dataset from 1951–2013 was used to study the return levels and precipitation extremes to keep extreme values more reliable and reasonable.

Monthly averaged data from the National Centers for Environmental Prediction-National Center for Atmospheric Research (NCEP-NCAR) reanalysis project were used to analyze the trends of meteorological variables. The dataset has a $2.5° \times 2.5°$ grid resolution at 17 pressure levels (Kalnay et al., 1996).

2.2 Methods

We adopted the top-value method to define EPEs. We sorted the precipitation data (≥ 0.1 mm) of each station and selected the top-*n* values. Based on this method, two types of EP time series were constructed. Type one is the EP amount. The top-1 precipitation (top-1P) and the accumulated value of the top-10 precipitation (top-10P) were selected. Six time series were constructed based on these two measures and the total precipitation (TPRE) at each station: annual top-1P, annual top-10P, annual TPRE, summer top-1P, summer top-10P, and summer TPRE (Table 1). Another type of time series is the total number of stations. Taking advantage of the denser stations, we sorted the daily precipitation data of the whole recorded period and counted the number of stations at which EPs occur in different regions for each year. Subsequently, time series of the total number of stations of top-1 and top-10 precipitation (top-1N and top-10N) were constructed, respectively, for the nation and each defined region. This type of

Table 1 Abbreviations and definitions of the EP time series

Short name	Definition
top-1P	annual maximum daily precipitation
top-10P	accumulated amount of annual top-10 maximum daily precipitation
summer top-1P	top-1P in summer
summer top-10P	top-10P in summer
annual TPRE	total annual precipitation
summer TPRE	total annual precipitation in summer
top-1N	annual total number daily top-1 precipitation stations for the whole recorded period in the Nation, NWC, NC, NEC, SE , SC, or SWC
top-10N	annual total number daily top-10 precipitation stations for the whole recorded period in the Nation, NWC, NC, NEC, SEC, SC, or SWC

time series has advantages; the occurrence frequency of top-10 precipitation at each station is the same for the same data time spans. For example, if the time span of the dataset is 50 yr, all 10 maximum precipitation events at each station have a 5-year return period. This type of time series ensures both the extreme nature and area coverage of EPEs; the time series of the total number of stations will therefore reflect real EP trends for each region.

To investigate regional EP characteristics, we divided China into six subregions, that is, Northeast China (NEC), North China (NC), Northwest China (NWC), Southwest China (SWC), Southeast China (SEC), and South China (SC; Figure 1). We considered both of the administrative boundaries of the provinces, autonomous regions and municipalities, and the spatial distribution of positive or negative trends of the annual top-1 daily precipitation to subjectively select these six subregions. The number of stations and coverage of each subregion are as follows: NEC contains 180 observation stations including Liaoning, Jilin, Heilongjiang, and the northeast of Inner Mongolia; NC includes 454 observation stations including Beijing, Tianjin, Hebei, Shanxi, the middle-east of Inner Mongolia, and the northern area of the Yellow River in the Henan and Shandong provinces; NWC contains Xinjiang, Gansu, Qinghai, Ningxia, Shanxi, and the west of Inner Mongolia (a total of 329 stations); SWC covers Sichuan, Chongqing, Guizhou, Yunnan, and Tibet (388 stations); SEC contains 434 stations including Hubei, Anhui, Jiangsu, Zhejiang, Jiangxi, Hunan, and Shanghai; and SC includes the Guangdong, Guangxi, Fujian, and Hainan provinces (240 stations). Taiwan, Hong Kong, and Macau are not included in these subregions due to the lack of continuous observational record available to us.

Two methods were employed to calculate the trends of the time series and test their statistical significance. For the time series of continuous variables, such as top-1P and top-10P, linear regression was used to assess trends. The trend results are represented as increase (decrease) ratio, which is defined as the ratio of the total trend value of the linear regression to the mean value of EPs within the trend period. The Mann-

Kendall method was used to test the statistical significance of the trends. For time series of discrete variables, that is, top-1N and top-10N, we used logistic regression to estimate the trends and test their statistical significance (Schmidli and Frei, 2005). The significance levels of the tests were set to 5%.

In most of the regions in China, summer (June to August) is the main precipitation season; therefore, we used the mean summer value to analyze the trends of atmospheric variables. We constructed a time series with four variables for each grid. The variables are the 500 hPa geopotential height, 850 hPa geopotential height, 850 hPa *v* wind (meridional wind), and 850 hPa specific humidity. Their trends and statistical significance test were also investigated using the above-mentioned methods (top-1P and top-10P). The results are represented as total increasing or decreasing trend values of the linear regression per 50 year.

Because the precipitation data span more than 50 yr, we can calculate the empirical return levels from these data to further evaluate the frequency of different precipitation extremes. Sample quantiles are defined as weighted averages of consecutive order statistics. Given a series of values $x_1, x_2, \cdots, x_n$, sort these values to form order statistics:

$$x_{(1)} \leq x_{(2)} \leq \cdots \leq x_{(n)}. \tag{1}$$

Then, use the order statistics as quantiles, which correspond to the fractions:

$$q_i = \frac{i-1}{n-1}, (i = 1, \cdots, n). \tag{2}$$

Given a quantile q, if q lies between q_i and q_{i+1}, define the qth quantile to be:

$$Q(q) = (1-f)Q(q_i) + fQ(q_{i+1}). \tag{3}$$

In detail, we sorted the precipitation data for the whole recorded period and each station. If the data period at a certain station is n years, we selected the top-*n* values and calculated the percentile based on the above-mentioned method. For example, precipitation occurring once in 50 yr means that the probability exceeding the percentile is 2% and that the probability of less than the percentile is 98%. We then calculated

the percentile based on the given probability.

The trends and return levels were computed with the R software package (Gilleland and Katz, 2011).

3. Extreme precipitation trends in China

3.1 Top-1P and top-10P trends

Figure 1a displays the spatial distribution of linear top-1P trends. Among the 2024 observation stations studied, 1225 stations (~61%) show increasing trends. The areas showing an increase are much larger than those displaying a decrease. Three regions show notable change: the SEC region showing a positive trend extends widely along the middle and lower reaches of the Yangtze River; the NWC region with a positive trend mainly includes Xinjiang, the western part of Gansu, north of Qinghai, and middle of Shanxi; and the NC region with a negative trend includes Hebei, Beijing, and Tianjin. The magnitudes of either increase or decrease ratio in most of the stations located in the above-mentioned three subregions (SEC, NWC and NC) reach 10–30% and are sometimes even larger than 30%. Linear trends are not as notable in the other three subregions. Positive trends were observed in NEC as whole; however, the trends are not notable at most of individual stations. The trends in SC are mainly positive; however, the ratios of change during the period are small, except for a few stations in the northern part of SC and Hainan Province. In SWC, notable increasing trends are observed in the central eastern areas of the Sichuan Basin, east of Guizhou, and in the middle of the Yunnan Province, whereas decreasing trends are recorded in the west and south of the Sichuan Basin and southeast of the Yunnan Province.

Among the 2024 observation stations, 145 stations (7.2%) pass the statistical significance test; 115 (40) stations of the 145 stations show a significant increase (decrease). The average increase (decrease) ratio is 38% (39%). The stations passing the statistical significance test are mainly located in the three subregions with notable trends (SEC, NWC and NC). The spatial distribution of the top-10P trends (Figure omitted) is very similar to that of top-1P. The positions with positive and negative trends do not greatly differ; the main differences lie in the trend distribution and intensity of stations passing the statistical significance test. The number of top-10P stations passing the statistical significance test significantly increases in the central western areas of NWC, especially in Xinjiang, but significantly decreases in the central northern areas of NC and east of SWC. The increase (decrease) ratios of top-10P are more notable in Xinjiang but have varying degrees in the central eastern areas of China. Among the 142 stations passing the statistical significance test for top-10P, 121 stations show positive trends with ratios increasing by 29% and 21 stations display negative trends with ratios de-
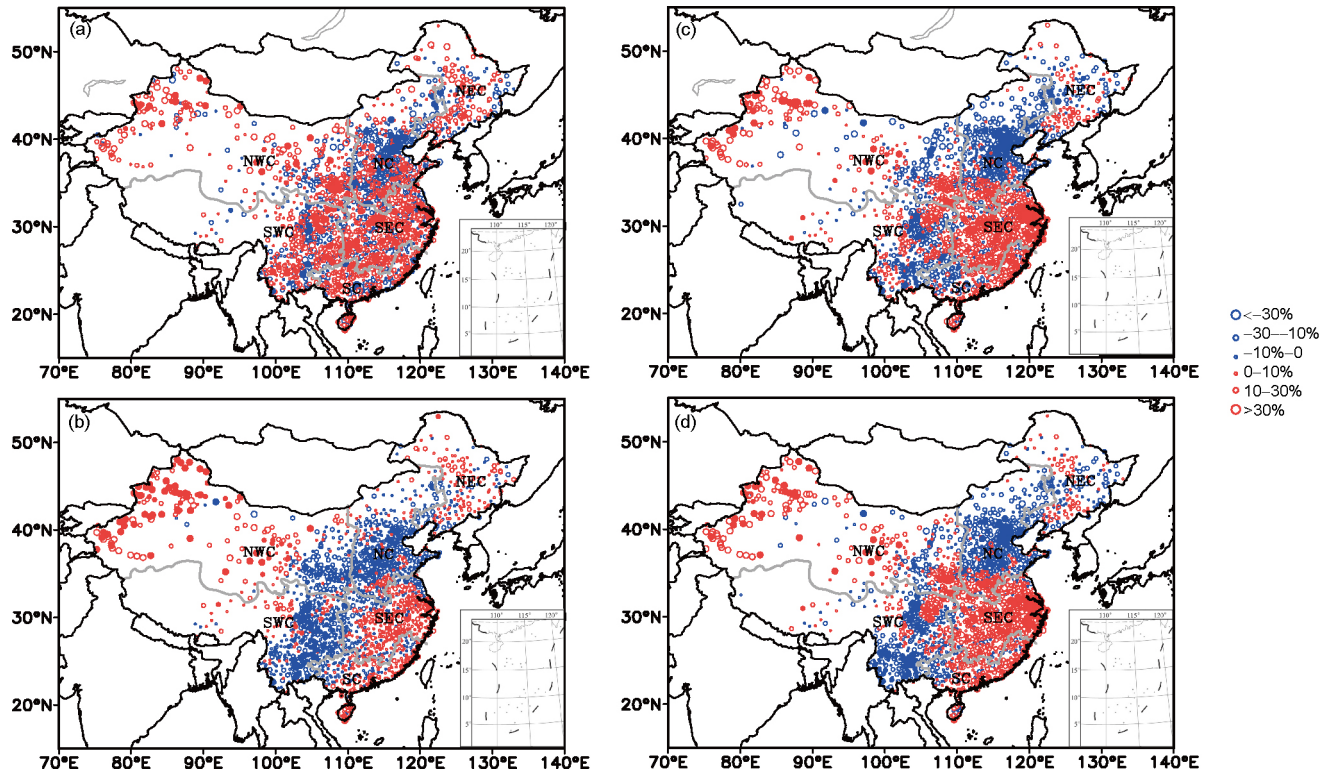
Figure 1   Spatial distribution of linear trends of the EP time series (represented as increasing/decreasing ratio in percent); the red (blue) dot shows the increasing (decreasing) trend; a solid (hollow) dot means passing (not passing) the statistical significance test with a significant level of 0.05; the thick grey lines are the region boundaries. (a) annual top-1P, (b) annual TPRE, (c) summer top-10P, (d) summer TPRE.

creasing by 25%, on average. The number of stations with a significant increase is much larger than that with a decrease, for both time series (top-1P and top-10P).

The annual TPRE trends include more negative stations compared with top-1P (Figure 1b), but the general spatial distribution patterns do not change, except for some regional features. The three obvious trend regions of top-1P are also observed for annual TPRE. The NWC region also shows notable increasing trends, especially in Xinjiang, but decreases are observed in the east of NWC. Most of the stations in SEC show positive trends compared with top-1P, but the increase ratios and number of stations passing the statistical significance test are reduced. Most areas with decreasing trends of annual TPRE are larger in NC, much larger than that of top-1P. The most notable differences between the trends of annual TPRE and top-1P were observed in the east of SWC and east of NWC. Most stations in these two areas, which are dominated by positive trends with respect to top-1P, show negative trends in the annual TPRE. Furthermore, more stations pass the statistical significance test for annual TPRE compared with top-1P. The opposite trends between top-1P and annual TPRE indicate that the proportion of EP of annual total precipitation increases. Thus, special attention must be paid to the east of NWC and east of SWC. The increase of annual TPRE in the middle and lower reaches of the Yangtze River are less notable than that of top-1P, which means that the EP increases much faster than the total precipitation. Figure 1b also shows that the areas with stations with negative trends are mainly situated in the second step terrains and their transition zones to plains.

The spatial trend patterns of summer top-1P and summer top-10P (Figure 1c) are similar to that of the annual top-1P. However, the intensity and coverage of the decreasing trends of summer top-10P in NC are much larger than that of annual top-1P. The trends of summer TPRE (Figure 1d) are in better agreement with the trends of annual top-1P, summer top-1P, and summer top-10P, especially in the east of NWC and Sichuan Basin. Negative trends or weak positive trends are observed for annual TPRE in these two areas; however, notable positive trends are observed for summer TPRE, which are consistent with that of annual top-1P and top-10P. Above all, the EP trends are in much better agreement with the trends of summer TPRE than with that of annual TPRE. This also means that the EP mainly occurs in summer. We also noticed inconsistencies between the EP trends and summer TPRE. For example, most of the stations with positive trends of annual top-1P are located in the middle and west of the Yunnan Province, but negative trends are observed for summer TPRE.

3.2   Top-1N and top-10N trends

The monthly distribution of the total number of stations with

EP from 1961 to 2013 for the whole country of China indicates that EPEs mainly occur from June to August. In July, the largest number of stations has EP, while August takes the second place. In fact, 84.8% (81.4%) of the national top-1N (top-10N) are observed in the summer season (Figure 2a and b). This result supports the conclusion mentioned above, that is, that the EP trends are in much better agreement with the summer TPRE trends.

Increasing trends are observed for both national top-1N (Figure 3a) and top-10N (Figure 3b). The P-values of the statistical significance test are both 0.03, passing the statistical significance test of the defined significance level of 0.05. The trends of national top-1N and top-10N on average increase by 2.4 and 15 stations per decade, respectively. The increase of the two time series becomes larger as time advances. The national top-1N and top-10N show very distinct interannual variations, with median values of 38 and 382 stations and standard variations of 13 and 94, respectively. Figure 3 shows that there have been three periods with highly frequent EPs since 1960: early 1960s, especially 1963; middle and late 1990s, mainly 1994–1998; and early 21st century, mainly 2010–2013. More discrete features have been observed in the trends of the national top-1N and top-10N since the mid-1990s. The years with an abnormal large number of stations have increased since 1993; therefore, a few of the years become off-group points in the box-whisker plot. For example, the annual mean national top-1N and top-10N are 34 and 355 stations, respectively, for the period of 1961–1993, compared with 46 and 427 stations for the period of 1994–2013 (Figure 3a and b). To determine if this result indicates that EPEs are likely to abnormally burst in certain years after 1990s, further research is required. Zhao et al. (2016) also showed that the frequency of EPs (>50, 100, 200 mm) significantly increases after the 1990s in the east of China.

The top 5 of the national top-1N are 70 stations in 1998 and 2010, 68 stations in 1994, 62 stations in 1996 and 2013, and 57 stations in 1963 and 2012. The least number of stations are 14 stations in 1986. The top 5 national top-10N are 621 stations in 1998, 534 stations in 2010, 529 stations in 1994, 510 stations in 1996, and 502 stations in 2012. The least number of stations are 267 stations in 1986 (the same year as for the national top-1N). The years with the top 5 number of national top-1N and top-10N are basically consistent. The years with a large number of top-1N and top-10N correspond to serious historic flooding events such as the floods in 1998 along the Yangtze River Basin and along the Nen-Songhua River Basin, floods in 2010 in the south of China and Jilin Province, the big flood in 1994 along the Pearl River Basin, flood of the Xijiang and Dongting Lake in 1996, torrential rainfall in NC in 2012, and the heavy rainfall event in the Sichuan Basin in 2013.

The increases of the national top-1N and top-10N are not always consistent with that of the regional top-1N (Figure
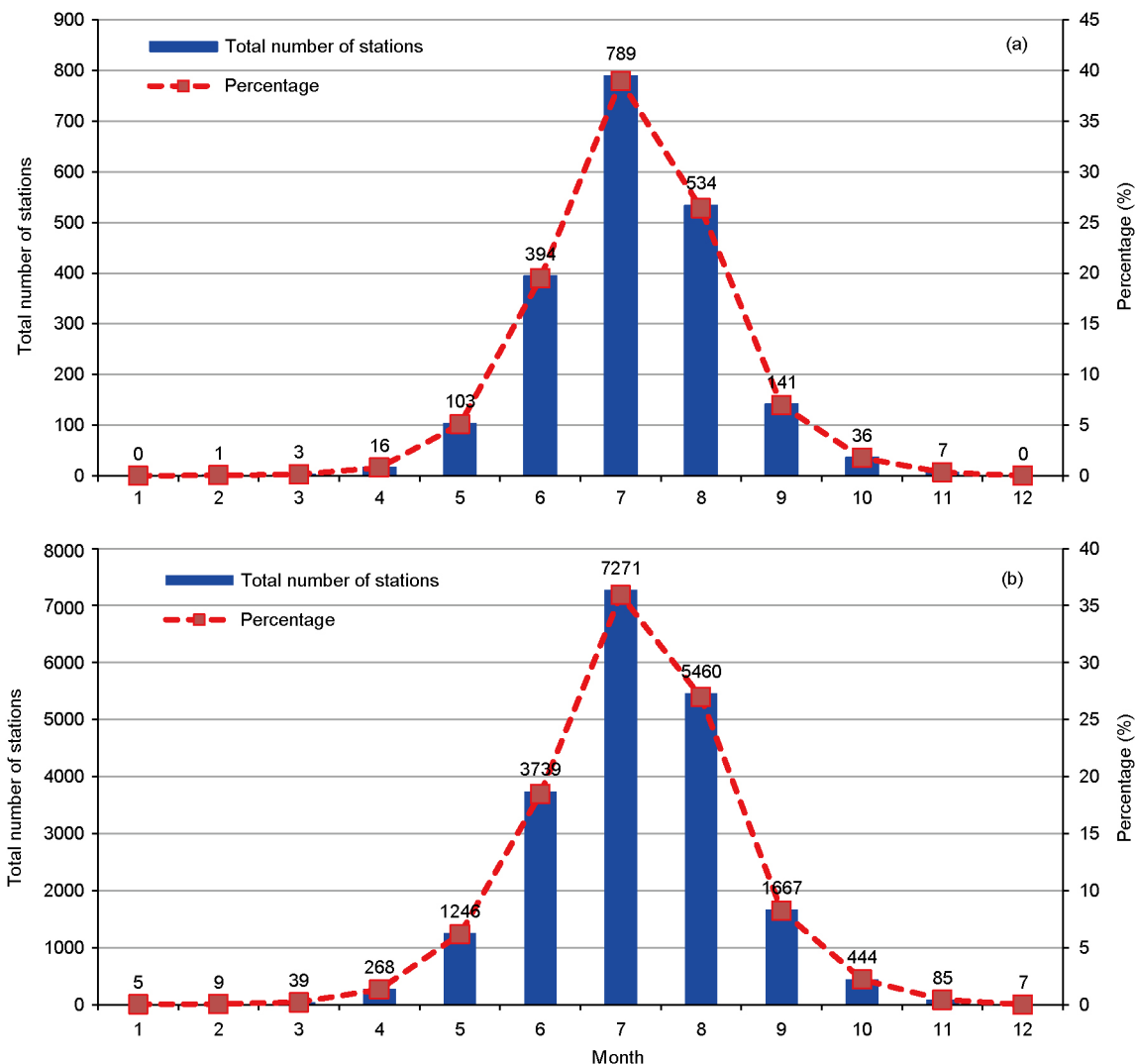
Figure 2   Monthly distribution of the total number of stations with EP. (a) Top-1, (b) top-10.

omitted) and top-10N (Figure 4). However, the change of the top-1N and top-10N in each region is consistent, that is, increase in each of the five regions and decrease in one region. The amplitude of the change in different regions differs. In NEC (Figure 4a), both top-1N and top-10N show insignificant increases. The trends in NC are both negative and insignificant (Figure 4b). Significant increases are observed in NWC, with top-1N and top-10N on average increasing by 1.2 and 5.2 stations per decade, respectively. Both trends pass the statistical significance test of the significance level of 5% (Figure 4c). The top-1N and top-10N in SWC (Figure 4) increased by 0.5 and 2.7 stations per decade, respectively, but the trends are not significant. The top-1N in SEC (Figure 4e) slightly (insignificantly) increases; however, the top-10N trend is notable and statistically significant, increasing by 5.8 stations per decade. Increasing trends are observed in SC for top-1N and top-10N, which on average increase by 0.57 and 2.9 stations per decade, respectively. The top-1N trend passes the statistical significance test; the top-10N trend does not

pass but has a relatively small P-value (0.05; Figure 4f). The analysis shows that the trends of the total number of stations are basically consistent with the EP trends in each region, that is, a region dominated by positive EP trends also shows an increase in the total number of stations and the region dominated by negative EP trends also displays a decrease in the total number of stations.

We selected 2024 stations nationwide and 10 maximum precipitations at each station to study the EP; thus, the average number of top-10N per year is 382 stations. If the number of top-10N in a certain year is greater than the normal average value, that year will experience more EP. The more top-10N stations are determined in a year, the more EP will occur in that year. The top-10N is higher than normal in 23 yr (Figure 5). The top three years are 1998, 2010, and 1994 with 382, 152, and 147 stations above normal, respectively. We also found that the EP often focuses on certain areas in abnormal years, for example, a higher number of top-10N is observed in NC in 1963 and 2000, in SEC in 1969, and in SC in 2006.
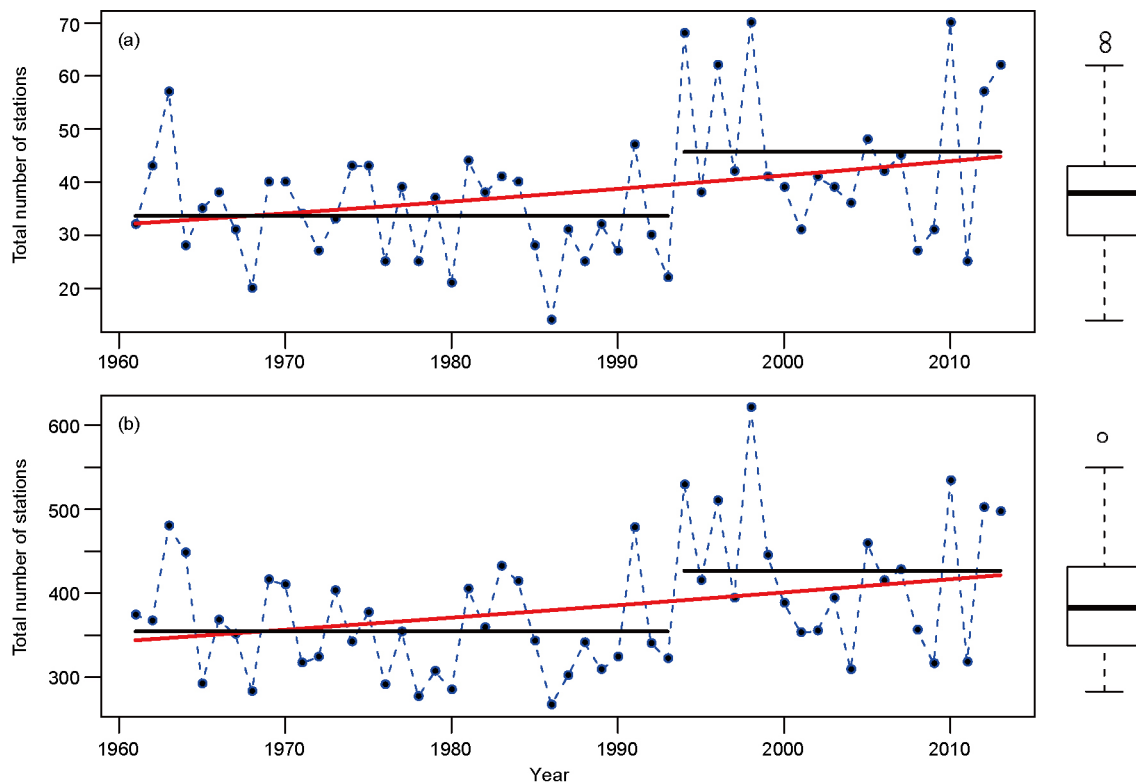
Figure 3   Time series and trend of the national total number of stations (right; the red line are trends; the black lines are the mean stations of the time periods from 1961–1993 and 1994–2013, respectively) and box-whisker plots of the number of stations (left; the thick lines in the box are medians; the thin lines at the box are the first and third quartile, respectively; the thin line at the whiskers are equal to or less than first and third quartile ± the 1.5 interquartile range (IQR) values; the IQR is the difference between the third and first quartiles). (a) Top-1N, (b) top-10N.
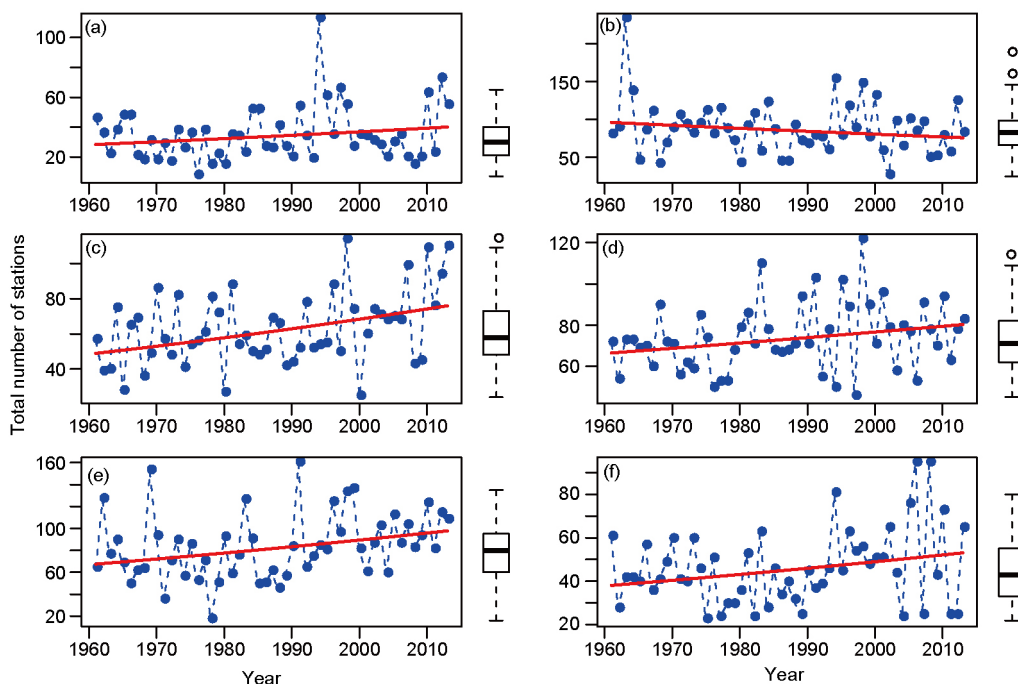
Figure 4   The same as Figure 3 but for the top-10 regional total number of stations. (a) NEC, (b) NC, (c) NWC, (d) SWC, (e) SEC, (f) SC.

As mentioned above, the time series of top-10N have three peak periods. Each period can be represented by the typical year of 1963, 1998, and 2010, respectively, which shows the highest number of stations in the respective period. The na-
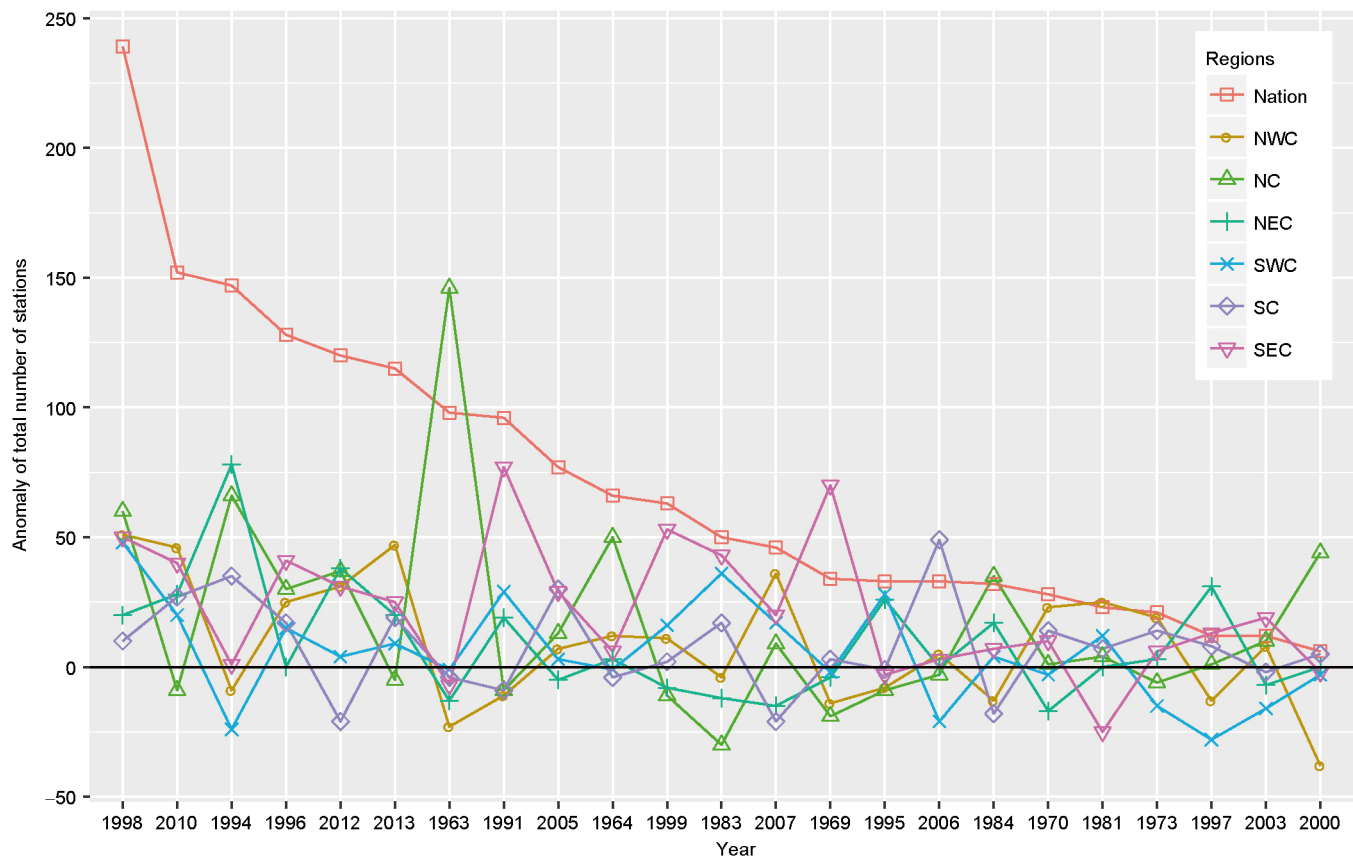
Figure 5   Sorted years of national top-10N, showing a positive anomaly and the corresponding regional top-10N anomaly.

tional top-10N is higher than normal at 98 stations in 1963 but much higher than normal at 146 stations in NC. This caused by the long-lasting "63.8" torrential rainfall event occurring in the middle and south of NC in August of 1963, which led to a large number of EP stations. The top-10N is smaller than normal in other regions in 1963. Serious floods struck China in 1998. The Yangtze River Basin and Nen-Songhua River Basin were the most seriously affected areas. Therefore, the highest number of national top-10N were observed in 1998; they were higher by 60, 51, 50, 48, 20, and 10 stations in NC, NWC, SEC, SWC, NEC. and SC, respectively. The year of 2010 is the year with the second highest number of national top-10N, the top-10N was smaller than normal by 9 stations in NC but higher than normal by 46, 40, 28, 27, 20 stations in NWC, SEC, NEC, SC, and SWC, respectively.

4.   Trend relations between atmospheric variables and EP in NC

Many factors may affect the spatial and temporal variations of EPEs. Climate change is one of the important factors. Physical arguments, empirical evidence, and global climate model (GCM) results all suggest that a warmer world likely will experience an increase in the frequency and magnitude of EPEs,

which are associated with a more intense hydrological cycle and increased water-holding capacity of the warmer atmosphere (Fowler and Hennessy, 1995). Satellite observations indicated that both precipitation and total atmospheric water have increased at approximately the same rate from 1987 to 2006, which is 7% per kelvin of surface warming (Wentz et al., 2007). However, our study shows that the EP trends and total number of stations in the east and north of NC decrease. Therefore, taking NC as example, we will further investigate the relations between the trends of atmospheric variables and the EP decrease. The weather conditions, which favor precipitation, are mainly the vertical movement of air and water vapor in the air. Temperature conditions can indirectly turn into water vapor conditions (Wentz et al., 2007). In our study, we selected several variables, which are related to precipitation dynamics and water vapor conditions: 500 and 850 hPa geopotential heights, 850 hPa *v* wind, and 850 hPa specific humidity. The time series of annual summer-averaged values of these variables were constructed at each grid point.

The linear trends of the 500-hPa and 850-hPa geopotential heights indicate the increase in China and nearby regions (Figure 6a and b). Areas showing the largest positive trend are located in the Mongolian Plateau and extend northeastward. Regions in which the geopotential height increases by
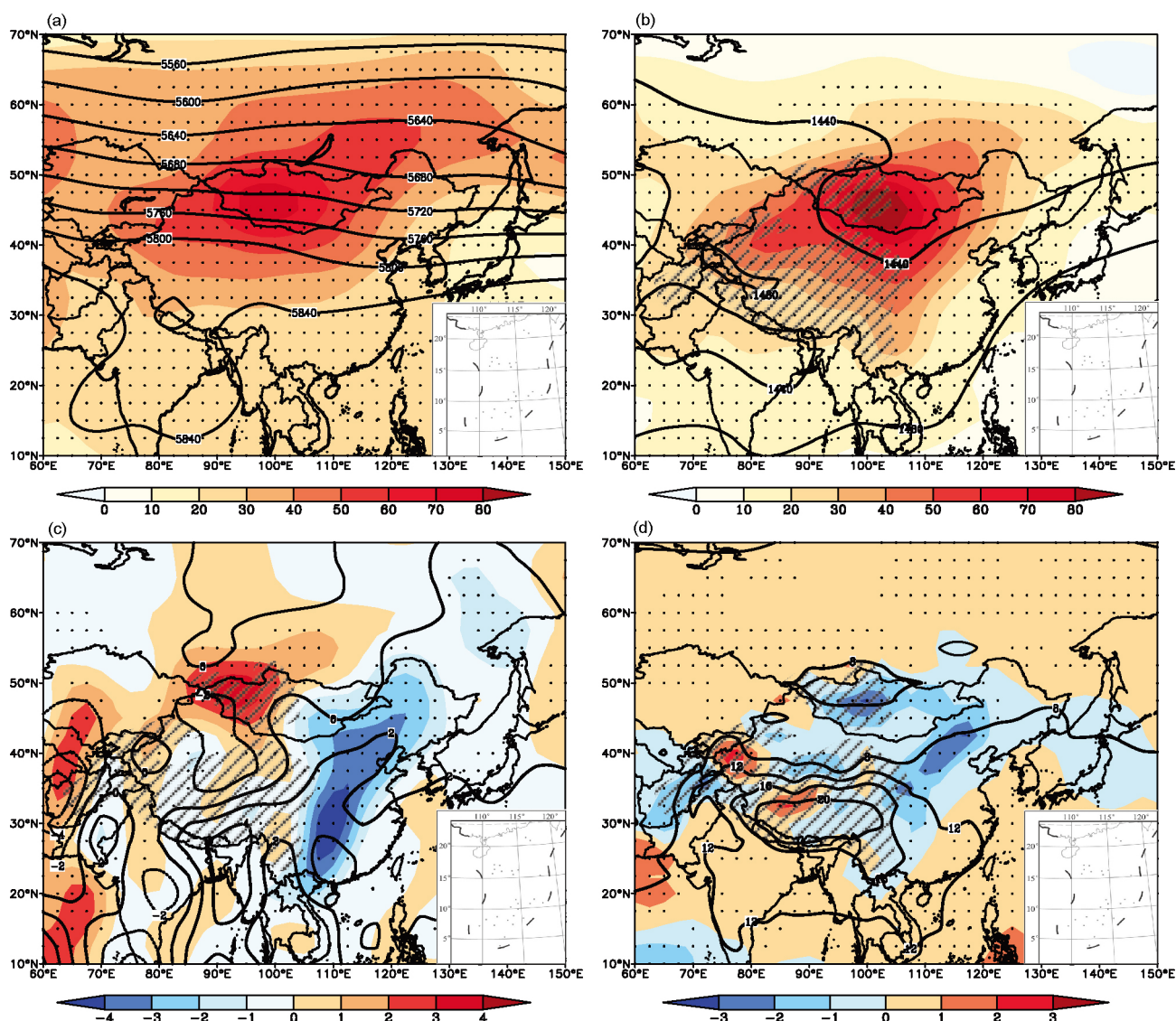
Figure 6   The total trend of increasing or decreasing values of the linear regression of atmospheric variables (shading area, unit: m; the contours are the mean values of the atmospheric variables from 1961–2013; the black dots are the grid points passing the statistical significance test; the area with the slant lines are terrains above 1500 m at 850 hPa), (a) 500 hPa geopotential height (m), (b) 850 hPa geopotential height (m), (c) 850 hPa *v* wind (m s^{-1}), (d) 850 hPa specific humidity (g kg^{-1}).

more than 30 m per 50 yr extend from Inner Mongolia to the east of NEC. Previous studies indicated that upper cold vortices are one of the main influencing systems during the summer precipitation periods in NC. Most of the heavy rainfall events in Beijing are caused by this type of circulation situation (Sun et al., 2005). An increasing geopotential height indicates the weakening of upper cold vortices and therefore the weakening of dynamic conditions triggering heavy rainfall. This may be one reason for the negative EP trends in NC.

In addition to above-mentioned dynamical conditions, decreasing trends in the water vapor transport and content are likely the other main causes of negative EP trends in NC. The 850 hPa *v* wind trends (Figure 6c) indicate that notable negative trends are observed over a large but narrow quasi-

meridional zone ranging from the south coast of China to the north of NC. The wind speed has decreased by more than 3 m s^{-1} per 50 yr. China is part of the East Asian monsoon region. The monsoon system moving northward to NC in July and August is responsible for the main precipitation season in NC. Northward transport of water vapor induced by a low-level southwest jet is the main source of water vapor for precipitation in NC. The decrease in *v* wind leads to a weakened northward transport of water vapor, which is also testified by areas with a negative trend of the specific humidity that overlap with areas with 850 hPa *v* wind. A notable negative trend center of 2–3 g kg^{-1} per 50 yr is seen in NC (Figure 6d).

Above all, the trends of the analyzed atmospheric variables indicate the increase of the geopotential height in NC and its

upstream regions and decrease of the low-level v wind and specific humidity in NC and its southwest areas. The increase of the geopotential height causes the weakening of the intensity of cold vortices and dynamic conditions triggering heavy precipitation. On the other hand, the decrease of the low-level v wind and specific humidity lead to the weakening water vapor content and transport. The changes of some atmospheric variables are favorable for EP decrease in NC. It is particularly important to note that we only explain the causes of the decreasing EP trends in NC in terms of some atmospheric variables directly affecting the precipitation. In this paper, we will not discuss other indirect factors such as the air temperature, westerlies, subtropical high, South Asia high, and climate-affecting factors.

5. Empirical return level of extreme precipitation

Another important purpose of trend analysis is to estimate the frequency and recurrence of the precipitation extremes. The return period and return level are two most important variables for this purpose. They are not only used for decision-making in water conservancy planning, bridge construction, house building, and insurance but are also very significant for routine operations in weather forecasting. Based on the analysis of the return period and level, the extremes of a certain precipitation event can be estimated and appropriate forecasting service measurements may be performed by forecasters. The return period and level are inversely related and have a one-to-one correspondence. According to the method introduced in Section 2.2, the return period will be $1/p$ if the probability exceeding a percentile or threshold for selected data is p. For example, a 50-year return level gives one precipitation amount in 50 yr; on the contrary, one different precipitation amount in 50 yr at different stations will correspond to the same 50-year return period. Here, we will only analyze the extreme event return level.

The spatial distribution of the empirical return level analyzed using real observation data is shown in Figure 7. The 20-year return levels gradually decrease from the southeast to the northwest of China (Figure 7a). The return levels are below 50 mm in the Tibetan Plateau and the middle and west of NWC. The values are 50–100 mm in the north of NEC,

Inner Mongolia Plateau, Loess Plateau, and Western Yunnan Province. In the south of NC, North China Plain, and south of the Qinling Mountains and Huaihe, the values are generally above 100 mm. Values >200 mm and locally even >300 mm are mainly distributed in the coastal areas of SEC and SC. The largest value, observed at the Xisha Station in the Hainan Province, is 462 mm. Values of 200–300 mm were also observed in several scattered areas inland. These areas are in good agreement with the local topography such as the Tongbai and Dabie mountains in the south of Henan and northeast of Hubei, Huangshan Mountains in the south of Anhui, Huaiyu Mountains in the northeast of Jiangxi, Wuling Mountains in the northwest of Hunan, and Longmen and Daba mountains in the northern and western Sichuan Basin. The spatial distribution features of the 50-year return levels are very similar to that of the 20-year return levels but have larger distribution values. The 50-year return levels are 400–600 mm at the south coast; they gradually reduce to 10–50 mm in NWC (Figure 7b). Here, we define the increasing rate as the value of 50-year return levels minus the 20-year return level divided by the 20-year return level. The mean increasing rate is 6.8%, which is less than 20% at 76% of the stations and can reach more than 100% at most (Figure 7c).

The historical maximum daily precipitation reflects the highest EP in history. This precipitation value is certainly greater than the 50-year empirical return levels. The maximum values can reach more than 100 mm in the east of the Greater Khingan Range, Inner Mongolia Plateau, and Qinghai-Tibet Plateau (Figure 7d). The west sides with >200 mm precipitation include the mountains of Yanshan, Taihang, Funiu, Wudang, Wushan, and Daloushan and the east of the Yunnan-Guizhou Plateau. The distribution of >300 mm precipitation is closely related to the local terrain mentioned above, while large coastal values are mainly related to typhoon precipitation. Based on the comparison of the precipitation maxima in six regions and the 50-year empirical return levels, the maximum precipitation can reach more than twice the 50-year empirical return levels. As of 2013, the precipitation maximum at all national stations is 755 mm, which is due to the "75.8" torrential rain in the Henan Province; the corresponding 50-year empirical return level is 354 mm (Table 2).

Table 2 Maximum daily precipitation in six regions and corresponding 50-year empirical return level[a]

Regions	Maximum daily precipitation (mm)	Date	Station (ID)	50-year empirical return level (mm)
NWC	304	08-29-2003	Ningshan, Shanxi (57137)	116
NC	755	08-07-1975	Shangcai, Henan (57194)	354
NEC	414	08-04-1958	Dandong, Liaoning (54497)	244
SEC	539	07-12-1994	Yangxin, Hubei (58500)	201
NC	645	08-30-2001	Qingyuan, Guangdong (59280)	294
SWC	525	07-29-1993	Ermei, Sichuan (56384)	360

a) The date is the ending observation time of daily precipitation.
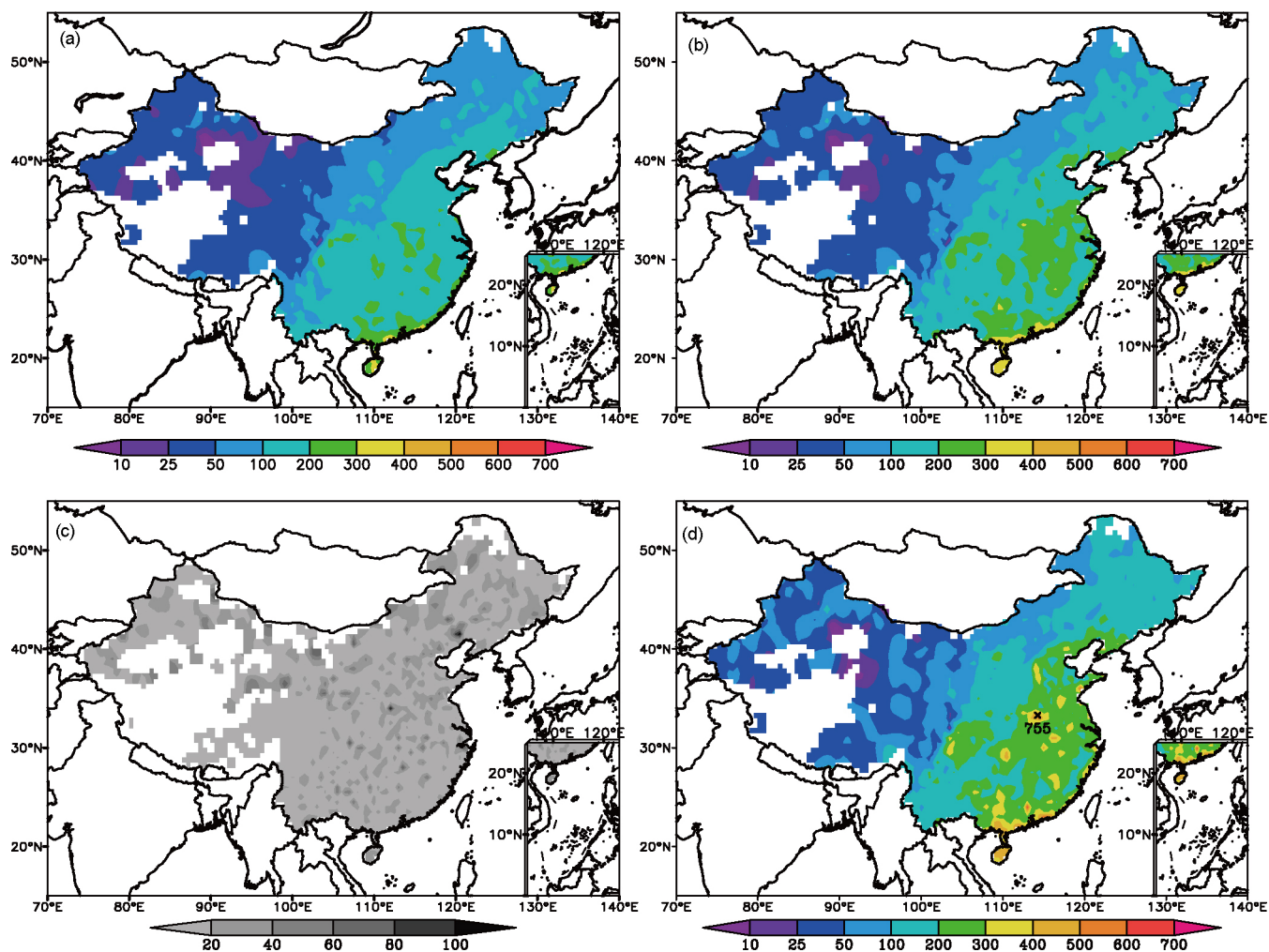
Figure 7   (a) 20-year empirical return levels (unit: mm), (b) 50-year empirical return levels (unit: mm), (c) 50-year empirical return level increase rates compared with the 20-year empirical return level (%), (d) historical daily maximum precipitations (unit: mm).

6.   Conclusions and discussion

Examination of the trends of the time series of annual top-1 precipitation, accumulated top-10 precipitation, summer top-1 precipitation, and accumulated summer top-10 precipitation indicates that there are three significant trend regions of EP over China: a positive trend region in SEC widely extending along the middle and lower reaches of the Yangtze River; a positive trend region in NWC, mainly containing Xinjiang, west of Gansu, north of Qinghai, and middle of Shanxi; a negative trend region in NC including Hebei, Beijing, and Tianjin. The ratios of changes (either increase or decrease) of 10–30% or even >30% were observed in these three regions. In other regions, the trends are insignificant or the change ratios are small. The EP trends are not consistent with the trends of the total annual precipitation but agree better with the trends of the total summer precipitation.

Increasing trends were observed for the time series of the national top-1N and top-10N. The number of stations on average increases by 2.4 and 15 stations per decade, respectively,

but with great interannual variations. There have been three periods with a large amount of EP stations since 1960: the early 1960s, middle and late 1990s, and early 21st century. The maximum number of stations of these time series was observed in 1998. The trends of regional top-1N and top-10N show differences. The most significant increase was observed in NWC. In SEC, the top-1N trends change steadily, but a notable top-10N increase was observed. In the SC, the two time series show a significant increase. The trends of the two time series in NEC and SWC are slightly increasing. An insignificant decrease of the two time series was observed in NC. The trends of the total number of stations are basically consistent with the EP trends in each region.

The trends of the atmospheric variables indicate an increase in the geopotential height in NC and its upstream regions and decrease in the low-level *v* wind and specific humidity in NC and its southwest areas. The increase of the geopotential height reflects the weakening of the intensities of upper cold vortices and dynamic conditions triggering heavy precipitation. On the other hand, the decrease of the low-level *v* wind

and specific humidity lead to the decrease of the water vapor content and transport. The changes of these atmospheric variables favor the EP decrease in NC.

The 50-year empirical return levels are 400–600 mm at the south coast and gradually reduce to <50 mm in NWC. The mean increasing rate is 6.8% compared with the 20-year empirical return levels; historical maximum precipitation can be more than twice the 50-year empirical return levels.

This study only focuses on the daily precipitation and interannual variations. We did not analyze the extremes and trends of long-lasting heavy precipitation processes and short-duration heavy precipitation. We did not discuss the decadal variations of the trends. The causes of the EP trends are complex and vary in different regions. Changes of the atmospheric circulation, atmospheric thermal conditions, and climate factors may all impact the EP trends. Taking NC as example, we here only discussed the causes of decreasing EP trends in this region in terms of atmospheric variables directly affecting the precipitation. The atmospheric thermal conditions may indirectly affect the atmospheric water vapor content (Wentz et al., 2007), which is note discussed here.

References

Allan R P, Soden B J. 2008. Atmospheric warming and the amplification of precipitation extremes. Science, 321: 1481–1484

Bissolli P, Friedrich K, Rapp J, Ziese M. 2011. Flooding in eastern central Europe in May 2010—Reasons, evolution and climatological assessment. Weather, 66: 147–153

Cao L, Pan S. 2014. Changes in precipitation extremes over the "Three-River Headwaters" region, hinterland of the Tibetan Plateau, during 1960–2012. Quat Int, 321: 105–115

Chen H P. 2013. Projected change in extreme rainfall events in China by the end of the 21st century using CMIP5 models. Chin Sci Bull, 58: 1462–1472

Chen H S, Fan S D, Zhang X H. 2009. Seasonal differences of Variation characteristics of extreme precipitation events over China in the last 50 years (in Chinese). Trans Atmos Sci, 32: 744–751

Chen Y, Sun J, Xu J, Yang S N, Zong Z P, Chen T, Fang C, Sheng J. 2012. Analysis and thinking on the extremes of the 21 July 2012 torrential rain in Beijing. Part I: Observation and thinking (in Chinese). Meteorol Monther, 38: 1255–1266

Du H, Xia J, Zeng S. 2014. Regional frequency analysis of extreme precipitation and its spatio-temporal characteristics in the Huai River Basin, China. Nat Hazards, 70: 195–215

Du J, Grumm R H, Deng G. 2014. Ensemble anomaly forecasting approach to predicting extreme weather demonstrated by extremely heavy rain event in Beijing (in Chinese). Chin J Atmos Sci, 38: 685–699

Fan L, Lu C H, Yang B, Chen Z. 2012. Long-term trends of precipitation in the North China Plain. J Geogr Sci, 22: 989–1001

Feng G L, Gong Z Z, Zhi R. 2010. Latest advances in climate change detection techniques. Acta Meteorol Sin, 24: 1–16

Fowler A M, Hennessy K J. 1995. Potential impacts of global warming on the frequency and magnitude of heavy precipitation. Nat Hazards, 11: 283–303

Gilleland E, Katz R W. 2011. New software to analyze how extremes change over time. Eos Trans AGU, 92: 13–14

Gochis D, Schumacher R, Friedrich K, Doesken N, Kelsch M, Sun J, Ikeda K, Lindsey D, Wood A, Dolan B, Matrosov S, Newman A, Mahoney K, Rutledge S, Johnson R, Kucera P, Kennedy P, Sempere-Torres D, Steiner M, Roberts R, Wilson J, Yu W, Chandrasekar V, Rasmussen R, Anderson A, Brown B. 2015. The great Colorado flood of September 2013. Bull Amer Meteorol Soc, 96: 1461–1487

Grams C M, Binder H, Pfahl S, Piaget N, Wernli H. 2014. Atmospheric processes triggering the central European floods in June 2013. Nat Hazards Earth Syst Sci, 14: 1691–1702

Houze Jr R A, Rasmussen K L, Medina S, Brodzik S R, Romatschke U. 2011. Anomalous atmospheric events leading to the summer 2010 floods in Pakistan. Bull Amer Meteorol Soc, 92: 291–298

Huang J, Sun S, Xue Y, Li J, Zhang J. 2014. Spatial and temporal variability of precipitation and dryness/wetness during 1961–2008 in Sichuan Province, West China. Water Resour Manage, 28: 1655–1670

Jiang F, Hu R J, Wang S P, Zhang Y W, Tong L. 2013. Trends of precipitation extremes during 1960–2008 in Xinjiang, the Northwest China. Theor Appl Climatol, 111: 133–148

Kalnay E, Kanamitsu M, Kistler R, Collins W, Deaven D, Gandin L, Iredell M, Saha S, White G, Woollen J, Zhu Y, Leetmaa A, Reynolds R, Chelliah M, Ebisuzaki W, Higgins W, Janowiak J, Mo K C, Ropelewski C, Wang J, Jenne R, Joseph D. 1996. The NCEP/NCAR 40-year reanalysis project. Bull Amer Meteorol Soc, 77: 437–471

Lau W K M, Wu H T, Kim K M. 2013. A canonical response of precipitation characteristics to global warming from CMIP5 models. Geophys Res Lett, 40: 3163–3169

Lynch S L, Schumacher R S. 2014. Ensemble-based analysis of the May 2010 extreme rainfall in Tennessee and Kentucky. Mon Weather Rev, 142: 222–239

Martius O, Sodemann H, Joos H, Pfahl S, Winschall A, Croci-Maspoli M, Graf M, Madonna E, Mueller B, Schemm S, Sedláček J, Sprenger M, Wernli H. 2013. The role of upper-level dynamics and surface processes for the Pakistan flood of July 2010. Q J R Meteorol Soc, 139: 1780–1797

Min S, Qian Y F. 2008. Trends in all kinds of precipitation events in China over the past 40 years (in Chinese). Acta Sci Nat Univ Sunyatseni, 3: 105–111

Moore B J, Neiman P J, Ralph F M, Barthold F E. 2012. Physical processes associated with heavy flooding rainfall in Nashville, Tennessee, and vicinity during 1–2 May 2010: The role of an atmospheric river and mesoscale convective systems. Mon Weather Rev, 140: 358–378

Pendergrass A G, Hartmann D L. 2014. Changes in the distribution of rain frequency and intensity in response to global warming. J Clim, 27: 8372–8383

Ren D. 2014. The devastating Zhouqu storm-triggered debris flow of August 2010: Likely causes and possible trends in a future warming climate. J Geophys Res-Atmos, 119: 3643–3662

Schmidli J, Frei C. 2005. Trends of heavy precipitation and wet and dry spells in Switzerland during the 20th century. Int J Climatol, 25: 753–771

Solomon S D, Qin D H, Manning M, Chen Z, Marquis M, Averyt K B, Tignor M, Miller H L. 2007. Climate Change 2007: The Physical Science Basis. Contribution of Working Group I to the Fourth Assessment Report of the Intergovernmental Panel on Climate Change. Cambridge: Cambridge

University Press. 945–946

Su B D, Jiang T, Jin W B. 2006. Recent trends in observed temperature and precipitation extremes in the Yangtze River basin, China. Theor Appl Climatol, 83: 139–151

Sun J, Chen Y, Yang S N, Dai K, Chen T, Yao R, Xu J. 2012. Analysis and thinking on the extremes of the 21 July 2012 torrential rain in Beijing. Part II: Preliminary causation analysis and thinking (in Chinese). Meteorol Monther, 38: 1267–1277

Sun J, Dai K, Fan L Q. 2011. Analysis and forecasting technology on the heavy rainfall processes in the Northeast China during July to August 2010 (in Chinese). Meteorol Monther, 37: 785–794

Sun J H, Zhang X L, Wei J, Zhao S X. 2005. A study on severe heavy rainfall in North China during the 1990s (in Chinese). Clim Environ Res, 10: 492–506

Sun J Q. 2012. The Contribution of extreme precipitation to the total precipitation in China . Atmos Ocean Sci Lett, 5: 499–503

Takahashi H G, Fujinami H, Yasunari T, Matsumoto J, Baimoung S. 2015. Role of tropical cyclones along the monsoon trough in the 2011 Thai flood and interannual variability. J Clim, 28: 1465–1476

Tang C, Rengers N, van Asch T W J, Yang Y H, Wang G F. 2011. Triggering conditions and depositional characteristics of a disastrous debris flow event in Zhouqu city, Gansu Province, northwestern China. Nat Hazards Earth Syst Sci, 11: 2903–2912

Tao S Y. 1980. Heavy Rainfalls in China (in Chinese). Beijing: Science Press. 1–3

Wang B L, Zhang M J, Wei J L, Wang S J, Li X F, Li S S, Zhao A F, Li X S, Fan J P. 2013. Changes in extreme precipitation over Northeast China, 1960–2011. Quat Int, 298: 177–186

Wang M, Guo P W, Wu Y. 2014. Variation characteristics of extreme precipitation in eastern China and its relationship with atmospheric stability (in Chinese). Trans Atmos Sci, 37: 47–56

Wang Q, Zeng B, Long Y Y. 2013. Diagnosis of the continuous rainstorm in Sichuan Basin during 7–11 July 2013 (in Chinese). J Anhui Agri Sci, 41: 12400–12404, 12408

Wentz F J, Ricciardulli L, Hilburn K, Mears C. 2007. How much more rain will global warming bring? Science, 317: 233–235

Yang J H, Jiang Z H, Yang Q G, Sun X Y, Yao Y B. 2007. Anlysis on extreme precipitation event over the Northwest China in flood season (in Chinese). J Desert Res, 27: 320–325

Yang T, Shao Q X, Hao Z C, Chen X, Zhang Z X, Xu C Y, Sun L M. 2010. Regional frequency analysis and spatio-temporal pattern characterization of rainfall extremes in the Pearl River Basin, China. J Hydrol, 380: 386–405

Zeng Y T, Lu E. 2015. Changes of summer rainfall and extreme precipitation during 1961–2010 in China. Progressus Inquisitiones De Mutatione Climatis, 11: 79–85

Zhai P M, Wang C C, Li W. 2007. A review on study of change in precipitation extremes (in Chinese). Adv Clim Change Res, 3: 144–148

Zhai P M, Zhang X B, Wan H, Pan X H. 2005. Trends in total precipitation and frequency of daily precipitation extremes over China. J Clim, 18: 1096–1108

Zhang A Y, Gao X, Ren G Y. 2008. Characteristic of extreme precipitation events change in central North China in recent 45 years (in Chinese). J Arid Meteorol, 26: 46–50

Zhang S Q, Ma Z F. 2011. Change tendency and cyclicity analysis of extreme precipitation over Sichuan province during 1961–2009 (in Chinese). J Nat Res, 26: 1918–1929

Zhao Y, Xu X D, Zhao T L, Xu H X, Mao F, Sun H, Wang Y H. 2016. Extreme precipitation events in East China and associated moisture transport pathways. Sci China Earth Sci, 59: 1854–1872

Zou Y C, Yang X Q, Sun X G, Tang J P, Fang J B, Liao Y F. 2009. Seasonal difference of the spatio-temporal variation of the number of the extreme precipitation processes in China (in Chinese). J Nanjing Univ-Nat Sci, 45: 98–108